Tuijin Jishu/Journal of Propulsion Technology
ISSN: 1001-4055
Vol. 46 No. 04 (2025)

Optimization of process parameters to improve Surface finish, MRR and dimensional accuracy while drilling SS410

M. Madusudanprasad, B. Sai Ram

ME Department, University College of Engineering Kakinada, JNTUK, Kakinada, India.

Abstract

In order to simultaneously optimize machining time, material removal rate (MRR), surface roughness, cylindricity, and dimensional accuracy, this study focuses on optimizing several drilling parameters for SS410 stainless steel, such as spindle speed, feed rate, and drill diameter. A Mannford VL-760 CNC vertical machining center was used for the experiments. Drill sizes of 12, 14, and 16 mm, spindle speeds between 500 and 1500 rpm, and feed rates between 0.03 and 0.15 mm/rev were among the input conditions. The Taguchi L27 orthogonal array is employed in the experimental design. Using Taguchi with Grey Relational Analysis, the best parameters were found to be 1000 rpm, 0.03 mm/rev feed, and a 16 mm drill. With these parameters, the machining time was 297 seconds, the diameter error was 0.1764 mm, the MRR was 15.92 mm^3/s, the cylindricity was 0.093 mm, and the surface roughness was 5.785 µm.

Keywords: Optimization, Drilling and Taguchi Grey analysis

1. Introduction

A class of steels with at least 10.5% chromium and corrosion resistance is known as stainless steel (SS). Just as there are numerous engineering and structural carbon steels that meet different weldability, toughness, and strength requirements, there is also a wide range of SS with better levels of strength and corrosion resistance. It results from the carefully controlled addition of alloying elements, each of which provides special strength and resistance to certain circumstances. Austenitic, ferritic, duplex, martensitic, and precipitation hardening stainless steel (PHSS) are the five main families of stainless steel grades that are now offered. Drilling is a subtractive manufacturing technique that uses a revolving cutting instrument called a drill bit to make round holes in solid materials. It is one of the most commonly used machining techniques in production, and it is an essential function in a variety of industries, including construction, medical devices, energy, automotive, and aerospace. When producing components that need to be fastened, fluid passed through, electrical routed, or integrated structurally, drilling is crucial. Hole quality is directly impacted by important drilling factors such spindle speed, feed rate, depth of cut, and coolant application. Cutting velocity is controlled by spindle speed, material removal is influenced by feed rate, hole depth each pass is determined by cut depth, and heat and friction are reduced by coolant. To achieve the appropriate hole size, surface finish, and tool life, these factors must be carefully chosen and controlled. The use SS410 drills to create high-performance products in order to determine the best machining settings, surface finish is taken up for the present work. Vignesh et al. [1] investigated the effects of AlTiN-coated and uncoated high-speed steel (HSS) drill bits on the machinability of SS410 stainless steel. Drilling experiments based on Taguchi's L16 orthogonal array assessed surface roughness, material removal rate (MRR), and ovality. The results showed that AlTiN-coated drill bits outperformed uncoated ones, reducing surface roughness and ovality by 48.5% and 2% respectively, while improving MRR by 23%. The coating contributed to enhanced tool performance by reducing friction and heat generation during drilling. Jayaganth et al. [2] explored the influence of drilling parameters and cutting fluids on the machinability of SS410 stainless steel. Using a Taguchi L9 array, drilling tests on 5 mm thick plates were conducted with HSS twist drills and various cutting fluids. Results indicated that increased cutting speed and decreased feed reduced surface roughness, while coconut oil as a cutting medium provided superior surface quality. The study identified optimum machining parameters for minimized roughness and enhanced efficiency, highlighting the relevance of environmental and process parameters in drilling performance. Pramod George et al. [3] investigates CNC dry milling of AISI 410 and AISI 420 martensitic stainless steels (MSS), materials known for high hardness and corrosion resistance but poor machinability. The study is divided into six experimental phases. It identifies that spindle speed and feed rate significantly influence surface roughness (Ra) and cutting force (Fc), with optimal results achieved at 1500 rpm, 30 mm/min feed, and 0.3 mm depth of cut (DOC). Multi-criteria optimization using Grey Relational Analysis (GRA) and predictive modeling through Response Surface Methodology (RSM) confirmed these findings. SEM analysis reveals minimal wear at low parameter values, while higher spindle speeds increase wear due to diffusion and thermal softening. MSS 420 consistently showed higher response values due to its elevated Cr and C content. Gökçe et al. [4] focused on the multi-response optimization of surface roughness and adhering workpiece material in drilling Custom 450 stainless steel. Utilizing Taguchi's L16 orthogonal array, the study examined the effects of cutting speed, feed rate, and drill geometry. Grey Relational Analysis and ANOVA identified feed rate as the most influential factor for surface roughness. Higher speeds minimized adhesion and improved tool life. Mathematical models were developed using Response Surface Methodology for predictive analysis, confirming that optimal conditions significantly reduce roughness and material adhesion. Vignesh et al. [5] conducted a statistical evaluation of drilling parameters affecting SS410 stainless steel, focusing on surface roughness, MRR, and ovality. Using HSS drill bits and Taguchi's L16 design, the study revealed that high speed, low feed, and high point angle produced better surface finishes, while high speed and feed yielded better MRR. Analysis of variance showed feed rate as the dominant factor affecting surface roughness. Regression analysis confirmed the predictive capability of the model, demonstrating the effectiveness of systematic parameter optimization. Khanna et al. [6] examined sustainable machining practices for SS410 alloy to reduce power consumption and surface roughness. Through Taguchi's L27 design and RSM, experiments on both conventional and CNC machines evaluated the influence of cutting speed, feed, and depth of cut. The study emphasized the benefits of dry machining and identified feed rate as the most significant factor. The research advocated for energy-efficient machining in small and medium-sized enterprises by showcasing practical implementation of statistical and technological tools for sustainable manufacturing. Çiçek et al. [7] investigated the effects of deep cryogenic treatment and drilling parameters on surface roughness and roundness error during the drilling of AISI 316 stainless steel using M35 HSS twist drills. Utilizing the Taguchi method and multiple regression analysis, the study identified optimal cutting speed and feed rate parameters for minimizing surface imperfections. The experiments demonstrated that treated tools at 14 m/min cutting speed and 0.08 mm/rev feed rate yielded the best results, confirming the efficacy of Taguchi optimization for improving machining quality and efficiency. Sundeep et al.[8] optimized drilling parameters of AISI 316 stainless steel using Taguchi's methodology, focusing on the effects of spindle speed, feed rate, and drill diameter on surface roughness and material removal rate (MRR). Through ANOVA, the study established that cutting speed was the most influential factor for both surface finish and MRR. The findings underline the significance of parameter optimization in enhancing machining performance and minimizing tool wear and energy consumption during drilling. Rao et al. [9] employed artificial neural networks (ANNs) to predict cutting tool wear, surface roughness, and workpiece vibration during the boring of AISI 316 steel using cemented carbide inserts. The study used laser Doppler vibrometry and FFT analysis for signal acquisition and processing. By training multilayer perceptron models with experimental data, it demonstrated accurate predictions of machining responses, highlighting the effectiveness of ANN in modeling complex interactions in boring operations where tool vibration is significant.

2. Experimentation and Methodology:

SS 410 was used as the work piece material in the investigation. The mechanical characteristics and chemical makeup of the workpiece are given in Tables 1 and 2. The work piece utilized in this study is a rectangular block that is 180 mm long, 150 mm broad, and 20 mm thick. The experiments are carried out with HSS M2 Jobber drills with diameters of 12 mm, 14 mm, and 16 mm. The SS 410 work piece material and M2 drills are photographed in Fig. 1. A Mannford VL-760 CNC Vertical Machining Center, S&T (INDIA) is used for CNC drilling. The highest spindle speed is 8000 rpm, and the spindle motor has a power of 5.5 kW. Following drilling, the surface roughness was examined using an SJ210 Mitutoyo surface roughness tester, and the dimensional accuracy of the holes was examined using the Metris LKV 8.7.6 CMM, which has a measuring range of 800 x 700 x 600 mm. Every experiment is only carried out in rainy conditions. Taguchi technique is taken for optimizing drilling parameters of SS410 stainless steel.

Table 1 Chemical composition - MSS 410

Alloy	Cr	Ni	C	Mn	Si	Mo	P	Cu	Fe
AISI 410	11.94	0.519	0.131	0.816	0.36	0.24	0.024	0.077	Balance

Table 2 Annealed Mechanical Properties of MSS 410

Alloy	Tensile Strength (MPa)	Yield Strength (MPa)	Elongation (%)	Hardness (HRC)
AISI 410	510	290	34	38–45

Fig 1: SS 410 Workpiece Material and M2 drills

Using an L27 orthogonal array, the effects of spindle speed (A), feed rate (B), and drill diameter (C) on Material Removal Rate (MRR) and surface roughness were investigated using the Taguchi method. Feed rate had the most impact on MRR ("larger-is-better"), followed by diameter and speed. Higher feed and diameter greatly increased MRR; ideal parameters were 1500 rpm, 0.15 mm/rev, and 16 mm diameter. Diameter had the biggest impact on surface roughness ("smaller-is-better"), with better finish at faster speeds and smaller diameters. At 1500 rpm, 0.09 mm/rev, and 12 mm diameter, the best surface polish was achieved. The effects of spindle speed (A), feed rate (B), and tool diameter (C) on Material Removal Rate (MRR) and surface roughness were examined using Response Surface Methodology (RSM). At high feed and big diameter (1000 rpm, 0.15 mm/rev, 16 mm), MRR peaked at 32.08 mm^3/sec, whereas the lowest surface roughness (2.337 µm) happened at 1500 rpm, 0.09 mm/rev, and 12 mm diameter. RSM plots showed that the primary factors for MRR and roughness were feed rate and tool diameter, respectively. For balanced performance, moderate-to-high speed, moderate feed, and a smaller diameter were the ideal settings. In order to maximize MRR and minimize surface roughness, spindle speed (A), feed rate (B), and tool diameter (C) were optimized using an Artificial Neural Network (ANN) combined with a Genetic Algorithm (GA). The ANN correctly predicted responses after being trained on experimental data. With an anticipated MRR of 45.03 mm^3/sec and surface roughness of 4.03 µm, GA found that the ideal parameters were 1500 rpm, 0.15 mm/rev, and 16 mm diameter. This demonstrated a significant increase in MRR while preserving a respectable level of surface quality. For accurate machining process optimization that guarantees both performance and quality, the ANN-GA model worked well.

3. Results and discussions

3.1. Taguchi Method

The analysis of S/N ratios for machining time under the “smaller-is-better” condition, showed that feed rate had the highest influence (Delta = 5.89), followed by spindle speed (Delta = 4.10), while tool diameter had minimal effect (Delta = 0.13). Increasing feed from 0.03 to 0.15 mm/rev and speed from 500 to 1500 rpm significantly reduced machining time, improving S/N ratios from -49.80 to -43.91 and -48.67 to -44.56, respectively. Tool diameter showed negligible variation, with S/N ratios between -46.40 and -46.27. Interaction plots confirmed no significant interactions. Thus, feed and speed are important for minimizing time, with diameter having limited impact. Optimal machining time was achieved at high diameter (16 mm), high speed (1500 rpm), and high feed (0.15 mm/rev).

Table 3. Response Table for S/N Ratios of Time

Level	SPEED (A)	FEED (B)	DIA (C)
1	-48.67	-49.80	-46.40
2	-45.76	-45.28	-46.31
3	-44.56	-43.91	-46.27
Delta	4.10	5.89	0.13
Rank	2	1	3

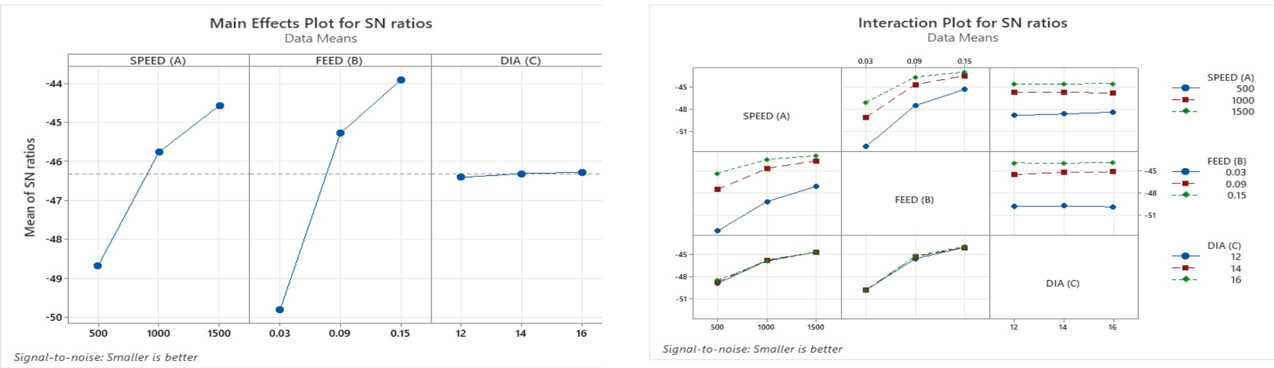

Figure 2 Main effects and Interaction Plots for SN Ratios of Time

3.1.1 Diameter error

The S/N ratio analysis for diameter error under the “smaller-is-better” condition, indicates that tool diameter (C) has the most significant influence (Delta = 7.76), followed by spindle speed (A) with Delta = 5.29, while feed rate (B) has the least effect (Delta = 1.39). As tool diameter increased from 12 mm to 16 mm, the S/N ratio decreased sharply from 20.99 to 13.22, indicating a rise in diameter error. Increasing spindle speed from 500 to 1500 rpm improved the S/N ratio from 15.58 to 20.87, suggesting reduced error at higher speeds. In contrast, feed showed only a mild variation across levels. Interaction plots reveal minor interactions, with tool diameter showing the strongest independent influence. Hence, to minimize diameter error, optimizing tool diameter and spindle speed is essential, whereas feed rate has limited impact. The optimum conditions of Dia error are occurred at 1500 rpm, 0.03mm/rev and 14mm tool diameter.

Table 4. Response Table for S/N Ratios of Dia Error

Level	SPEED (A)	FEED (B)	DIA (C)
1	15.58	18.38	19.31
2	17.07	18.15	20.99
3	20.87	16.99	13.22
Delta	5.29	1.39	7.76
Rank	2	3	1

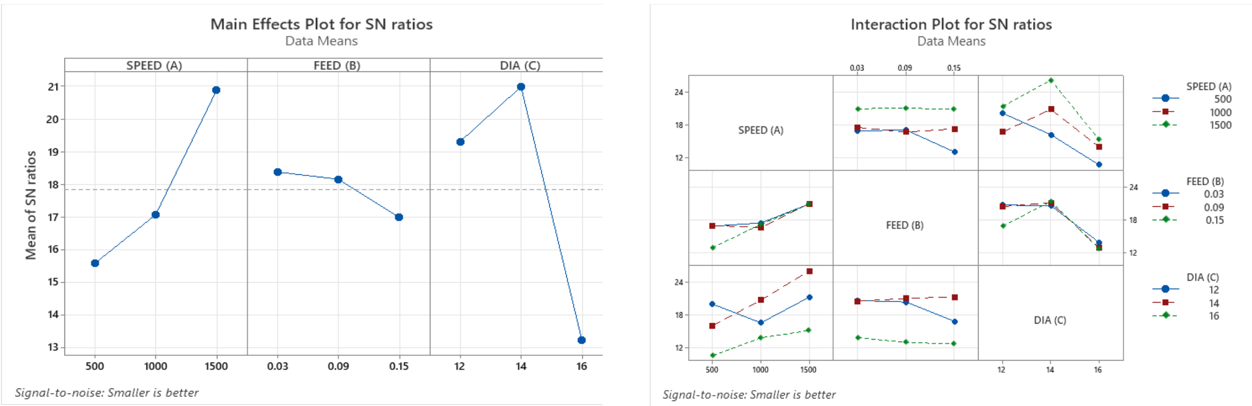

Figure 3 Main effects and Interaction Plots for SN Ratios of Dia Error

3.1.2 MRR

The signal-to-noise (S/N) ratio analysis for Material Removal Rate (MRR), based on the "larger-is-better" condition, revealed that feed rate (B) had the most significant influence (Delta = 5.93), followed by tool diameter (C) with Delta = 5.20, and spindle speed (A) with Delta = 4.00. As feed increased from 0.03 to 0.15 mm/rev, the S/N ratio improved markedly from 21.23 to 27.15, indicating a substantial rise in MRR. Similarly, increasing tool diameter from 12 mm to 16 mm raised the S/N ratio from 22.07 to 27.27, while spindle speed from 500 to 1500 rpm improved the S/N ratio from 22.43 to 26.43. Interaction plots showed consistent trends across levels with no strong interactions, suggesting that MRR improves independently with increasing feed, diameter, and speed. Therefore, the Optimal MRR was achieved at high diameter (16 mm), high speed (1500 rpm), and high feed (0.15 mm/rev).

Table 5 Response Table for S/N Ratios of MRR

Level	SPEED (A)	FEED (B)	DIA (C)
1	22.43	21.23	22.07
2	25.29	25.76	24.80
3	26.43	27.15	27.27
Delta	4.00	5.93	5.20
Rank	3	1	2

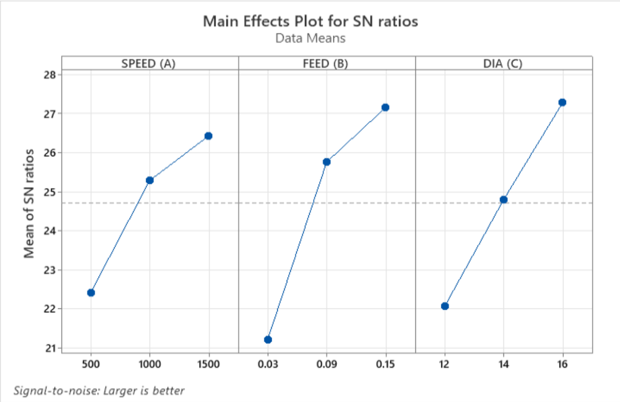

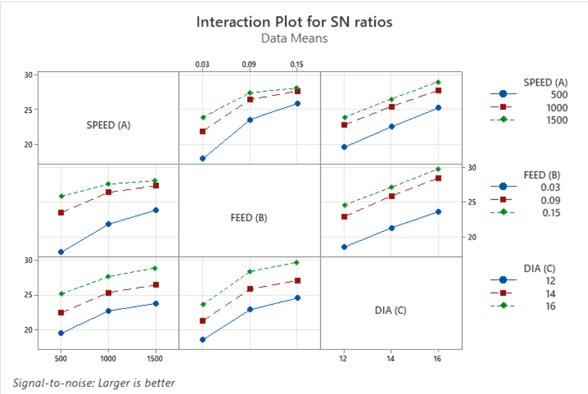

Figure 4 Main effects and Interaction Plots for SN Ratios of MRR

3.1.3 Cylindricity

The S/N ratio analysis for cylindricity error, under the "smaller-is-better" condition, revealed that tool diameter (C) had the highest influence (Delta = 7.78), followed by spindle speed (A) with Delta = 2.96, and feed rate (B) with the least impact (Delta = 2.52). As tool diameter increased from 14 mm to 16 mm, the S/N ratio dropped significantly from 36.59 to 28.80, indicating a sharp increase in cylindricity error. Spindle speed showed moderate variation, with the best result at 500 rpm (35.01), while feed rate showed a non-linear trend, peaking at 0.09 mm/rev (35.21). Interaction plots revealed that diameter interacts notably with feed and speed, affecting cylindricity error more sensitively. Overall, minimizing tool diameter is most effective in reducing cylindricity error, with spindle speed and feed playing secondary roles.

Table 6. Response Table for S/N Ratios of Cylindricity.

Level	SPEED (A)	FEED (B)	DIA (C)
1	35.01	33.10	35.60
2	32.05	35.21	36.59
3	33.92	32.68	28.80
Delta	2.96	2.52	7.78
Rank	2	3	1

Tuijin Jishu/Journal of Propulsion Technology
ISSN: 1001-4055
Vol. 46 No. 04 (2025)

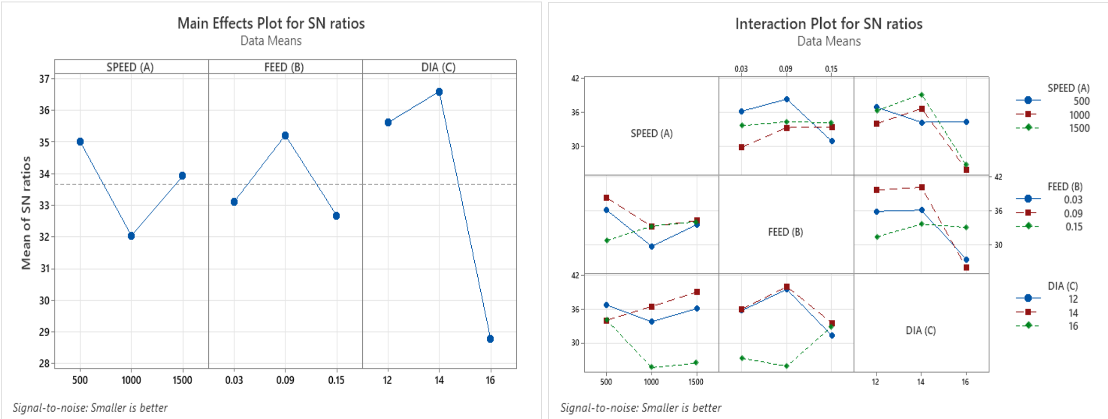

Figure 5 Main effects and Interaction Plots for SN Ratios of Cylindricity

3.1.4 Surface roughness

The S/N ratio analysis is under smaller is better, revealed that tool diameter (C) had the greatest influence on surface roughness with a delta of 5.685 and Rank 1. Surface finish deteriorated significantly as diameter increased from 12 mm to 16 mm (S/N from −9.34 to −15.03). Spindle speed (A) ranked second (delta = 1.630), with improved roughness at higher speeds (−11.66 at 500 rpm to −13.29 at 1500 rpm). Feed rate (B) showed the least effect (delta = 0.921), with a non-linear trend. Interaction plots confirmed strong interaction between speed and diameter. Optimal surface roughness was observed at 1500 rpm, 0.09 mm/rev, and 12 mm diameter.

Table 7. Response Table for S/N Ratios of Surface Roughness

Level	SPEED (A)	FEED (B)	DIA (C)
1	-11.664	-12.870	-9.343
2	-12.436	-11.949	-13.023
3	-13.294	-12.574	-15.028
Delta	1.630	0.921	5.685
Rank	2	3	1

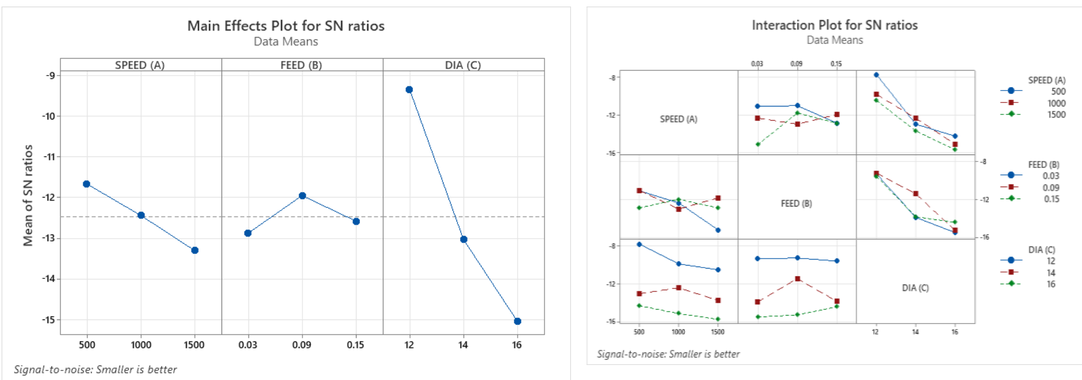

Figure 6 Main effects and Interaction Plots for SN Ratios of Surface Roughness

3.1.5 ANOVA

The significance of input parameters—spindle speed (A), feed rate (B), and tool diameter (C)—on various machining responses was evaluated using ANOVA at a 95% confidence level.

3.1.5.1 TIME

For machining time, feed rate (B) exhibited the highest influence ($F = 1505.04$, $P = 0.000$), followed by speed (A) ($F = 704.72$, $P = 0.000$). Tool diameter (C) showed no significant effect ($P = 0.513$). A significant interaction was found between speed and feed ($P = 0.000$), while other interactions were insignificant.

Table 8 ANOVA Table for Time

Source	DF	Seq SS	Adj SS	Adj MS	F	P
SPEED (A)	2	80.130	80.130	40.0648	704.72	0.000
FEED (B)	2	171.128	171.128	85.5640	1505.04	0.000
DIA (C)	2	0.083	0.083	0.0413	0.73	0.513
SPEED (A)*FEED (B)	4	10.199	10.199	2.5498	44.85	0.000
SPEED (A)*DIA (C)	4	0.260	0.260	0.0651	1.14	0.402
FEED (B)*DIA (C)	4	0.210	0.210	0.0525	0.92	0.496
Residual Error	8	0.455	0.455	0.0569		
Total	26	262.464				

3.1.5.2 DIA ERROR

In the case of diameter error, tool diameter (C) was the most significant factor ($F = 95.81$, $P = 0.000$), followed by speed (A) ($F = 42.79$, $P = 0.000$). The speed × diameter interaction was also statistically significant ($P = 0.001$), indicating notable coupled effects. Feed (B) and other interactions were statistically insignificant ($P > 0.05$).

Table 9 ANOVA Table for Dia Error

Source	DF	Seq SS	Adj SS	Adj MS	F	P
SPEED (A)	2	134.15	134.15	67.077	42.79	0.000
FEED (B)	2	10.07	10.07	5.034	3.21	0.095
DIA (C)	2	300.34	300.34	150.172	95.81	0.000
SPEED (A)*FEED (B)	4	22.01	22.01	5.502	3.51	0.062
SPEED (A)*DIA (C)	4	85.15	85.15	21.287	13.58	0.001
FEED (B)*DIA (C)	4	20.35	20.35	5.087	3.25	0.073
Residual Error	8	12.54	12.54	1.567		
Total	26	584.61				

3.1.5.3 MRR

For material removal rate (MRR), all three main factors significantly influenced the response: feed (B) (F = 1324.44, P = 0.000), diameter (C) (F = 935.20, P = 0.000), and speed (A) (F = 586.78, P = 0.000). Additionally, the speed × feed interaction was significant (P = 0.000), while other interactions were not.

Table 10 ANOVA Table for MRR

Source	DF	Seq SS	Adj SS	Adj MS	F	P
SPEED (A)	2	76.536	76.536	38.2678	586.78	0.000
FEED (B)	2	172.752	172.752	86.3761	1324.44	0.000
DIA (C)	2	121.982	121.982	60.9912	935.20	0.000
SPEED (A)*FEED (B)	4	10.679	10.679	2.6697	40.94	0.000
SPEED (A)*DIA (C)	4	0.398	0.398	0.0995	1.53	0.283
FEED (B)*DIA (C)	4	0.260	0.260	0.0649	0.99	0.463
Residual Error	8	0.522	0.522	0.0652		
Total	26	383.128				

3.1.5.4 CYLINDRICITY

For cylindricity, only tool diameter (C) had a statistically significant effect (F = 6.49, P = 0.021). Speed (A), feed (B), and all interaction terms yielded $P > 0.05$, indicating negligible influence on form accuracy.

Table 11 ANOVA Table for Cylindricity

Source	DF	Seq SS	Adj SS	Adj MS	F	P
SPEED (A)	2	40.47	40.47	20.24	0.81	0.477
FEED (B)	2	32.96	32.96	16.48	0.66	0.542
DIA (C)	2	323.33	323.33	161.66	6.49	0.021
SPEED (A)*FEED (B)	4	81.01	81.01	20.25	0.81	0.551
SPEED (A)*DIA (C)	4	140.73	140.73	35.18	1.41	0.313
FEED (B)*DIA (C)	4	214.21	214.21	53.55	2.15	0.166
Residual Error	8	199.24	199.24	24.90		
Total	26	1031.94				

3.1.5.5 SURFACE ROUGHNESS

For surface roughness, tool diameter (C) remained the only significant factor (F = 15.33, P = 0.002). Speed, feed, and all interactions had no significant effect (P > 0.3), confirming the dominance of diameter in machining duration under those conditions.

Table 12 ANOVA Table for Surface Roughness

Source	DF	Seq SS	Adj SS	Adj MS	F	P
SPEED (A)	2	11.971	11.971	5.985	1.23	0.343
FEED (B)	2	3.980	3.980	1.990	0.41	0.678
DIA (C)	2	149.642	149.642	74.821	15.33	0.002
SPEED (A)*FEED (B)	4	21.984	21.984	5.496	1.13	0.409
SPEED (A)*DIA (C)	4	6.192	6.192	1.548	0.32	0.859
FEED (B)*DIA (C)	4	10.110	10.110	2.527	0.52	0.726
Residual Error	8	39.038	39.038	4.880		
Total	26	242.916				

These findings emphasize the dominant roles of feed in material efficiency (MRR and time), diameter in geometric accuracy (diameter error and Cylindricity), and significant speed–feed interaction in performance outcomes.

3.2 TAGUCHI GREY RELATIONAL ANALYSIS

Grey relational study is a way of converting two or more output parameters into a single output parameter so as to change the multi-response problem into a single response one. In Taguchi, the S/N Ratios of Time, Diameter Error, Cylindricity and Surface Roughness are calculated under the Smaller is Better Condition and MRR is Calculated under Larger is Better Condition. To analyze the Thaguchi's grey relational analysis, the S/N of each response are listed in table 13, GRC and GRR are listed in table 14.

Table 13 S/N Ratios of Time, Dia Error, MRR, Cylindricity and Surface Roughness

S.No/ Parameters	S/N Ratios				
	Time	Dia Error	MRR	Cylindricity	Surface Roughness
1	-53.2552	23.4397	15.1491	38.2728	-3.9951
2	-53.1028	15.83117	18.08157	31.8692	-14.6318
3	-53.0643	11.22915	20.53591	38.0618	-14.6076
4	-48.1987	22.49877	20.21667	44.43697	-9.37285
5	-47.3098	16.85691	23.85249	43.74173	-9.95793
6	-47.0822	11.48606	26.50945	26.48443	-13.7951

7	-45.2014	14.14159	23.38755	27.61813	-9.82723
8	-45.6207	15.6398	25.56809	26.72598	-14.4015
9	-45.1536	9.083965	28.52848	37.92393	-14.3866
10	-49.005	16.66548	19.51334	33.51435	-10.8838
11	-49.005	20.54669	22.09611	34.9916	-10.9185
12	-49.4551	15.07003	24.04	20.63034	-15.2461
13	-44.6599	16.58304	23.8604	38.2728	-10.8987
14	-44.6599	20.36363	26.44364	35.9176	-12.361
15	-44.6599	12.86037	28.88999	25.36822	-15.7166
16	-43.5795	16.55378	24.9415	29.7891	-7.71927
17	-43.4052	21.32014	27.686	38.78604	-13.8146
18	-43.4052	13.65127	30.12347	31.18182	-14.3634
19	-47.1205	21.92735	21.30215	35.70312	-12.9496
20	-47.1205	25.27207	23.93195	41.31003	-16.0637
21	-47.0822	15.42686	26.40533	23.54357	-16.537
22	-43.6369	22.11368	24.78335	36.02686	-7.37317
23	-43.6369	25.96864	27.4104	40.53744	-11.8613
24	-43.6369	14.66126	29.86738	26.07287	-16.2073
25	-42.9844	19.87068	25.46904	36.77264	-11.068
26	-42.9226	27.07193	28.11729	35.39102	-13.1945
27	-42.9226	15.54047	30.56257	29.95146	-14.3933

Table 14 GRC and GRR of Time, Dia Error, MRR, Cylindricity and Surface Roughness

GRC					SUM	GRR	RANK
1	0.385186	0.333333	0.402877	0.333333	2.45473	0.490946	18
0.971349	0.571366	0.381753	0.514356	0.766975	3.205799	0.64116	10
0.964365	0.807419	0.434589	0.405775	0.764711	3.376859	0.675372	5
0.505371	0.401359	0.426904	0.333333	0.466758	2.133725	0.426745	27
0.464942	0.536412	0.534566	0.339952	0.48801	2.363882	0.472776	23
0.455611	0.789218	0.655342	0.67033	0.695773	3.266273	0.653255	7
0.390793	0.640068	0.517864	0.630102	0.483097	2.661924	0.532385	12
0.403592	0.578398	0.606771	0.661334	0.745969	2.996064	0.599213	11
0.389384	1	0.791178	0.407691	0.744648	3.332902	0.66658	6

0.548645	0.542607	0.410895	0.480218	0.525904	2.508269	0.501654	17
0.548645	0.439659	0.476513	0.453208	0.527437	2.445463	0.489093	20
0.576189	0.600397	0.54161	1	0.82928	3.547477	0.709495	1
0.375416	0.545319	0.534859	0.402877	0.526561	2.385033	0.477007	22
0.375416	0.443629	0.651696	0.437774	0.600262	2.508777	0.501755	16
0.375416	0.704284	0.821673	0.715292	0.8843	3.500965	0.700193	3
0.348088	0.546288	0.578245	0.565154	0.415606	2.453382	0.490676	19
0.344048	0.423642	0.728197	0.395998	0.697281	2.589166	0.517833	14
0.344048	0.66321	0.946095	0.530101	0.742599	3.226053	0.645211	8
0.457157	0.411862	0.454215	0.441254	0.636105	2.400592	0.480118	21
0.457157	0.357158	0.537528	0.365323	0.929813	2.646979	0.529396	13
0.455611	0.586428	0.649591	0.80338	1	3.49501	0.699002	4
0.349438	0.408377	0.571464	0.436022	0.406287	2.171588	0.434318	26
0.349438	0.347544	0.709716	0.374196	0.572863	2.353757	0.470751	24
0.349438	0.61724	0.917258	0.686234	0.950051	3.520221	0.704044	2
0.334668	0.454685	0.602076	0.424427	0.534151	2.350007	0.470001	25
0.333333	0.333333	0.759134	0.446419	0.65231	2.524529	0.504906	15
0.333333	0.582116	1	0.560831	0.745235	3.221515	0.644303	9

4. Conclusion

This study focused on the optimization of drilling parameters—namely spindle speed, feed rate, and drill diameter—to improve multiple quality characteristics of SS410 components, specifically targeting surface roughness, material removal rate (MRR), dimensional accuracy (as diameter error), cylindricity, and machining time. From the Taguchi method, optimal parameters were identified with a spindle speed of 1000 rpm, feed of 0.03 mm/rev, and a 16 mm diameter drill, which together resulted in a machining time of 297 s, diameter error of 0.1764 mm, MRR of 15.92 mm^3/s, cylindricity of 0.093 mm, and surface roughness of 5.785 µm. However, further multi-objective optimization using Grey Relational Analysis (GRA) refined these outputs, enhancing the optimization across all responses simultaneously. These optimized settings and methodologies are directly applicable to industries seeking improved productivity, dimensional accuracy, and surface integrity in stainless steel machining.

REFERENCES

[1] Vignesh, V., Satish, S., Gopi, V., Jishnoop, J., & Menon, G. A. (2022). Comparison of coated and uncoated HSS drill bit on surface roughness, material removal rate and dimensional accuracy of SS410 stainless steel. Materials Today: Proceedings, 58, 13–19. https://doi.org/10.1016/j.matpr.2021.12.307

[2] Jayaganth, A., Jayakumar, K., Deepak, A., & Pazhanivel, K. (2018). Experimental studies on drilling of 410 stainless steel. Materials Today: Proceedings, 5, 7168–7173. https://doi.org/10.1016/j.matpr.2017.11.382

[3] George, P. (2022), Philip Selvaraj D. Experimental investigations on CNC dry milling of AISI 410 and AISI 420 martensitic stainless steels (Doctoral dissertation, Karunya Institute of Technology and Sciences). http://hdl.handle.net/10603/508716

[4] Vignesh, V., Ilangovan, S., & Radhika, N. (2021). Statistical analysis of process parameters in drilling of SS410 stainless steel. Materials Today: Proceedings, 46, 3313–3319. https://doi.org/10.1016/j.matpr.2020.11.470

[5] Gökçe, H., & Çiftçi, İ. (2023). Mathematical modelling and multiresponse optimization to minimize surface roughness in drilling Custom 450 stainless steel. Manufacturing Technologies and Applications, 4(1), 11–24. https://doi.org/10.52795/mateca.1238328

[6] Kilickap, E., Huseyinoglu, M., & Yardimeden, A. (2011). Optimization of drilling parameters on surface roughness in drilling of AISI 1045 using response surface methodology and genetic algorithm. The International Journal of Advanced Manufacturing Technology, 52(1–4), 79–88. https://doi.org/10.1007/s00170-010-2710-7

[7] Jayaram Reddy, P., & Vinodh, D. (2023). Machining of aluminium 6063 alloy using high strength steel and titanium nitride novel coated drill tool using CNC and comparing the material removal rate. Journal of Physics: Conference Series, 2484(1), 012037. https://doi.org/10.1088/1742-6596/2484/1/012037

[8] Kamboj, A., Kumar, S., & Singh, H. (2015). Burr height and hole diameter error minimization in drilling of AL6063/15%/SiC composites using HSS step drills. Journal of Mechanical Science and Technology, 29(7), 2837–2846. https://doi.org/10.1007/s12206-015-0612

[9] Jayaram Reddy, P., & Vinodh, D. (2022). Material removal rate comparison of aluminium alloy 6063 machined using HSS tool and novel chromium nitride coated drill tool in CNC drilling. Materials Today: Proceedings, 69, 848–852. https://doi.org/10.1016/j.matpr.2022.07.284

[10] Ibrahim, G. A., Burhanuddin, Y., & Emrijakto, D. (2020). A study on drill machining for Magnesium alloy using Taguchi method. IOP Conference Series: Materials Science and Engineering, 857, 012014. https://doi.org/10.1088/1757-899X/857/1/012014

[11] Krishnan, V. K., John, V. J., & Girimurugan, R. (2023). Optimization of drilling parameters in vertical machining centre drilling on magnesium AZ91D alloy under dry condition with Taguchi design. Materials Today: Proceedings. https://doi.org/10.1016/j.matpr.2023.08.121

[12] Tzotzis, A., Antoniadis, A., & Kyratsis, P. (2024). Multivariate modelling of AA6082-T6 drilling performance using RSM, ANN and response optimization. International Journal of Lightweight Materials and Manufacture, 7, 531–545. https://doi.org/10.1016/j.ijlmm.2024.04.002

[13] Tsao, C. C., & Hocheng, H. (2008). Evaluation of thrust force and surface roughness in drilling composite material using Taguchi analysis and neural network. Journal of Materials Processing Technology, 203(1–3), 342–348. https://doi.org/10.1016/j.jmatprotec.2006.04.126

[14] Santhosh, A. J., Tura, A. D., Jiregna, I. T., Gemechu, W. F., Ashok, N., & Ponnusamy, M. (2021). Optimization of CNC turning parameters using face centred CCD approach in RSM and ANN-genetic algorithm for AISI 4340 alloy steel. Results in Engineering, 11, 100251. https://doi.org/10.1016/j.rineng.2021.100251

[15] Djurović, S., Lazarević, D., Ćirković, B., Mišić, M., Ivković, M., Stojčetović, B., Petković, M., & Ašonja, A. (2024). Modeling and prediction of surface roughness in hybrid manufacturing–milling after FDM using artificial neural networks. Applied Sciences, 14(14), 5980. https://doi.org/10.3390/app14145980

[16] Assarzadeh, S., & Ghoreishi, M. (2008). Neural-network-based modeling and optimization of the electro-discharge machining process. International Journal of Advanced Manufacturing Technology, 39, 488–500. https://doi.org/10.1007/s00170-007-1235-1

[17] Alduroobi, A. A. A., Ubaid, A. M., Tawfiq, M. A., & Elias, R. R. (2020). Wire EDM process optimization for machining AISI 1045 steel by use of Taguchi method, artificial neural network and analysis of variances. International Journal of System Assurance Engineering and Management. https://doi.org/10.1007/s13198-020-00990-z

[18] Babu, K. K., Panneerselvam, K., Sathiya, P., Haq, A. N., Sundarrajan, S., Mastanaiah, P., & Srinivasa Murthy, C. V. (2017). Parameter optimization of friction stir welding of cryorolled AA2219 alloy using artificial neural network modeling with genetic algorithm. International Journal of Advanced Manufacturing Technology, 97, 1–13. https://doi.org/10.1007/s00170-017-0897-6

[19] Çiçek, A., Kıvak, T., & Ekici, E. (2013). Optimization of drilling parameters using Taguchi technique and response surface methodology (RSM) in drilling of AISI 304 steel with cryogenically treated HSS drills. Journal of Intelligent Manufacturing, 25(2), 1–12. https://doi.org/10.1007/s10845-013-0783-5

[20] Kazeem, R. A., & Jen, T.-C. (2024). Performance assessment of Jatropha seed oil as lubricant during turning of AISI 1525 steel using Taguchi-grey relational analysis methodology. International Journal on Interactive Design and Manufacturing (IJIDeM). https://doi.org/10.1007/s12008-024-02112-6

[21] Sarıkaya, M., & Yılmaz, V. (2016). Optimization and predictive modeling using S/N, RSM, RA and ANNs for micro-electrical discharge drilling of AISI 304 stainless steel. Neural Computing and Applications. https://doi.org/10.1007/s00521-016-2775-9

[22] Shirmohammadi, M., Goushchi, S. J., & Keshtiban, P. M. (2021). Optimization of 3D printing process parameters to minimize surface roughness with hybrid artificial neural network model and particle swarm algorithm. Progress in Additive Manufacturing, 6, 199–215. https://doi.org/10.1007/s40964-021-00166-6

[23] Kilickap, E., & Huseyinoglu, M. (2010). Selection of optimum drilling parameters on burr height using response surface methodology and genetic algorithm in drilling of AISI 304 stainless steel. Materials and Manufacturing Processes, 25(10), 1068–1076. https://doi.org/10.1080/10426911003720854

[24] Mondal, N., Mandal, S., & Mandal, M. C. (2019). FPA-based optimization of drilling burr using regression analysis and ANN model. Measurement. Advance online publication. https://doi.org/10.1016/j.measurement.2019.107327

[25] https://extrudesign.com/how-drilling-machine-works-different-types/